

Control Design for Planar Bi-Rotor Helicopter Stabilization

Cesar Santoyo, and Claudia Ciaschi

Abstract—This paper discusses our implementation of a controller which stabilizes a bi-rotor helicopter. The planar Bi-Rotor Helicopter dynamics can be described by the provided equations of motion. First, we linearize the system about the origin. Next, we design, test, and compare two controllers, a linear feedback controller and a linear adaptive feedback controller. These controllers are then tested on the full system dynamics. Lastly, we design and test an adaptive controller to stabilize the full system dynamics.

I. INTRODUCTION

For this project we chose to address the dynamics of a bi-rotor planar helicopter. Step 1 addressed the issue of linearization of the dynamics, design and comparison of two different controllers, verification of the linearized system's stability, and the implementation of a linear adaptive controller under model mismatch parameters. Step 2 called for the transformation of the full system dynamics to control an offset point above the planar helicopter. Additionally, in Step 2, we augment our MRAC controller to address the general form of a system with nonlinear terms in the span of the input space. During both of these phases we constraint the control inputs to 6 times the baseline force (i.e., 6 times gravity).

Our project efforts are contained in this report and organized as follows:

- Section II contains the mathematical description of the full system dynamics.
- Section III presents the linearized version of the system which allows us to understand in first approximation its behavior. Here, we present and analyze the design of two controllers.
- Section IV discusses the results of the closed-loop system analysis, when the two controllers designed in Section III are applied to the full system dynamic (i.e., nonlinear system).
- Section V presents the transformation of the equations of motions to obtain a compact equation describing the full system. Then, it discusses the design of an adaptive controller able to stabilize this system.
- Section VI summarizes the conclusions.

Furthermore, the authors would like to note that all of the images in this file are 300 dpi and while their size is reduced due to space constraints, zooming into the report will allow for closer inspection of the plots without graphical distortion of the content. Lastly, some of the equations were shrunk due to space constraints.

C. Santoyo (csantoyo@gatech.edu) and C. Ciaschi (cciaschi3@gatech.edu) are with the School of Electrical & Computer Engineering, Georgia Institute of Technology, Atlanta, GA, 30318, USA.

II. SYSTEM DYNAMICS

Consider a bi-rotor helicopter whose dynamics are described as follows

$$m \begin{Bmatrix} \ddot{x} \\ \ddot{y} \end{Bmatrix} = -d \begin{Bmatrix} \dot{x} \\ \dot{y} \end{Bmatrix} + \begin{Bmatrix} -\sin(\theta) \\ \cos(\theta) \end{Bmatrix} \{1 \ 1\} \vec{f} - m \vec{g}$$

$$J \ddot{\theta} = r \{1 \ -1\} \vec{f}$$

where m is the mass of the helicopter, d is the mass flow rate, $\vec{g} = [0 \ g]^T$ is Earth's gravitational acceleration, r is the distance from the center of the force to the center of gravity of the helicopter, and J is the moment of inertial of the planar helicopter.

Additionally, the variables x , y , and θ are the x and y coordinates of the center of mass of the system, and its orientation, respectively. \vec{f} is the force vector applied in the body frame of the helicopter, and \vec{f} is the controller of the system. Each coordinate of $\vec{f} \in \mathbb{R}^2$ can be independently controlled; however, the force of the fans can't act in a "negative direction" unless the entire body has been flipped. In other words, the propellers only provide uni-directional thrust. As previously mentioned, the control inputs (i.e., propeller thrust) can't exceed 6 times the hover force.

We convert the system states to traditional state-space form as follows: $x_1 = x$, $x_2 = \dot{x}_1 = \dot{x}$, $x_3 = y$, $x_4 = \dot{x}_3 = \dot{y}$, $x_5 = \theta$, $x_6 = \dot{x}_5 = \dot{\theta}$ which renders the system dynamics as shown in (1).

$$\begin{bmatrix} \dot{x}_1 \\ \dot{x}_2 \\ \dot{x}_3 \\ \dot{x}_4 \\ \dot{x}_5 \\ \dot{x}_6 \end{bmatrix} = \begin{bmatrix} x_2 \\ -\frac{d}{m}x_2 - \frac{\sin(x_5)}{m}(f_1 + f_2) \\ x_4 \\ -\frac{d}{m}x_4 + \frac{\cos(x_5)}{m}(f_1 + f_2) - g \\ x_6 \\ \frac{r}{J}(f_1 - f_2) \end{bmatrix}$$

$$= \underbrace{\begin{bmatrix} x_2 \\ -\frac{d}{m}x_2 \\ x_4 \\ -\frac{d}{m}x_4 - g \\ x_6 \\ 0 \end{bmatrix}}_{\text{Natural Dynamics}} + \underbrace{\begin{bmatrix} 0 \\ -\frac{\sin(x_5)}{m}(f_1 + f_2) \\ 0 \\ \frac{\cos(x_5)}{m}(f_1 + f_2) \\ 0 \\ \frac{r}{J}(f_1 - f_2) \end{bmatrix}}_{\text{Control Portion}}$$
(1)

III. LINEARIZED SYSTEM WITH LINEAR CONTROL

We linearize the system about the point $x_5 = \theta = 0$, by performing the following operation

$$A = \left. \frac{\partial f}{\partial x} \right|_{x_5=0}.$$

The full system then becomes

$$\dot{x} = Ax + Bu$$

where A , B , and u are defined as follows

$$A = \begin{bmatrix} 0 & 1 & 0 & 0 & 0 \\ 0 & -\frac{d}{m} & 0 & 0 & -\frac{f_1(0)+f_2(0)}{m} \\ 0 & 0 & 0 & 1 & 0 \\ 0 & 0 & 0 & -\frac{d}{m} & 0 \\ 0 & 0 & 0 & 0 & 0 \\ 0 & 0 & 0 & 0 & 1 \end{bmatrix} \quad (2)$$

$$B = \begin{bmatrix} 0 & 0 \\ 0 & 0 \\ 0 & 0 \\ \frac{1}{m} & \frac{1}{m} \\ 0 & 0 \\ \frac{r}{J} & -\frac{r}{J} \end{bmatrix}$$

$$u = \begin{bmatrix} f_1 \\ f_2 \end{bmatrix}.$$

The values $f_1(0), f_2(0)$ are initial conditions on f , calculated at $x_5 = 0$. The forces are defined as a function of the angle, since angular offsets lead to lateral motion. Lastly, it is worth noting that the left propeller force \vec{f}_l and right propeller force \vec{f}_r relate to f_1 & f_2 as follows

$$f_1 = \|\vec{f}_r\| \text{ and } f_2 = \|\vec{f}_l\|.$$

Furthermore,

$$\vec{f}_r = \begin{cases} f_1 \sin(\theta) \\ f_1 \cos(\theta) - g \end{cases}$$

$$\vec{f}_l = \begin{cases} f_2 \sin(-\theta) \\ f_2 \cos(-\theta) - g \end{cases} = \begin{cases} -f_2 \sin(\theta) \\ f_2 \cos(\theta) - g \end{cases}$$

where $f_1(0), f_2(0)$ are found by setting $\theta = \theta_0$, where θ_0 is the initial orientation of the system.

A. Linear Controller

The linear controller (LQR) used to stabilize the system is of the following form

$$u = \begin{cases} f_1 \\ f_2 \end{cases}^1 = -K * x(t)$$

where K is the gain matrix able to stabilize the system. The matrix K is found using the MATLAB 'care()' built-in function.

The simulation results of the linearized dynamics with the LQR controller are shown in Fig. 1 and Fig. 2. The same controller is tested on the system with parameters offset by 15-20% where stability is also achieved. With and without parameter variation we see that stability is still achieved for the linearized dynamics.

¹ f_1 and f_2 are set to be no greater than 6 times the force of gravity, as requested from the project instructions

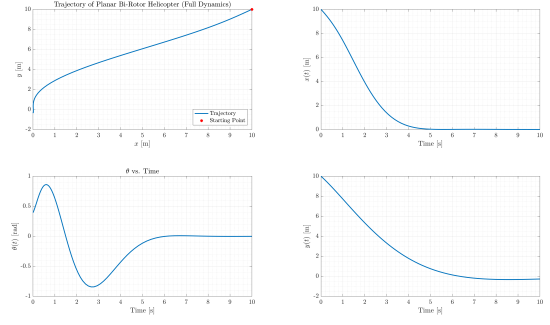


Fig. 1. Bi-Rotor Helicopter Response using an LQR controller. The system has been stabilized and converges at the origin.

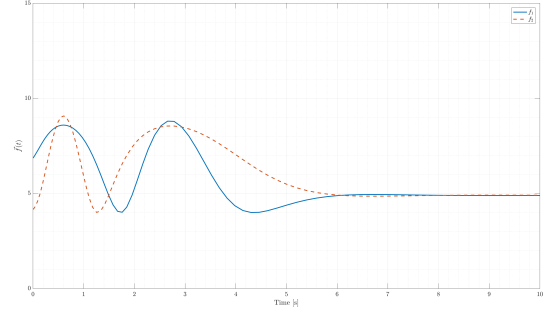


Fig. 2. Thrust force over time of Bi-Rotor Helicopter using an LQR controller. It is evident that the thrust utilized to stabilize the system does not exceed 6 times the baseline force (i.e., 6 times gravity).

B. Adaptive Controller

The peculiarity of an adaptive controller is that it not only is able to stabilize the closed-loop system, but it also provides tracking between the system trajectory and a desired signal of interest. This is important because with this controller, the helicopter is able to follow a specific desired trajectory, and to remain stable when this trajectory changes over time.

The closed-loop adaptive control system can be fully characterized by the following equations

$$\begin{aligned} \text{Plant: } & \dot{x} = Ax + Bu \\ \text{Reference: } & \dot{x}_m = A_m x + B_m u \\ \text{Controller: } & u = k_x^T x + k_r^T r(t) \\ \text{Adaptation Laws: } & \dot{k}_x = -\Gamma_x x e^T P B \text{sign}(\lambda) \\ & \dot{k}_r = -\Gamma_r r(t) e^T P B \text{sign}(\lambda) \end{aligned}$$

where, A and B are defined in Eq. 2 with offset parameters of 10-20% from the given nominal values, and B_m is the nominal B defined in Eq. 2 (i.e. no offset parameters). Next, $A_m = A - B k_x^{*T}$ from the matching conditions, and k_x & k_r are the adaptation laws, whose initial values are derived from the matching conditions. The matrices Γ_x and Γ_r are the adaptive gains and are positive semi-definite. The error, $e = x - x_m$, describes the quality of the tracking. The matrix $P \succ 0$ is found by solving the Riccati Equation where with $Q \succ 0$ is the identity matrix of appropriate dimensions. Lastly, $r(t)$

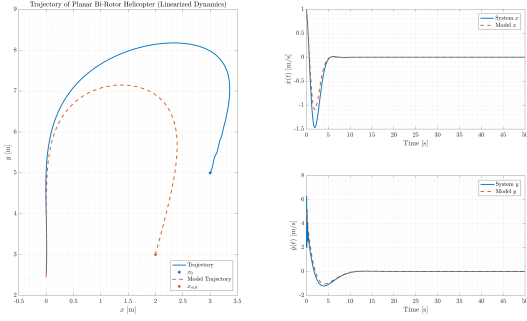


Fig. 3. Bi-Rotor Helicopter Response using a linear adaptive controller and constant $r(t)$. The system has been stabilized and tracking is achieved.

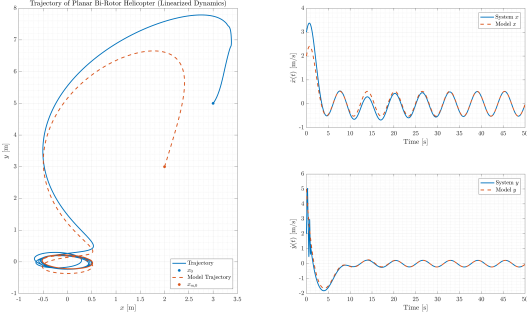


Fig. 4. Bi-Rotor Helicopter Response using a linear adaptive controller and sinusoidal $r(t)$. The system has been stabilized and tracking is achieved.

is the reference signal (i.e., the trajectory we aim to track with our adaptive controller).

In this section, we study the following three cases

- Tracking a linear trajectory where $r(t)$ is constant.
- Tracking a circular trajectory where $r(t)$ is a sinusoidal.
- Tracking a changing over time trajectory, $r(t)$ is the following sequence of signals

$$\begin{aligned} r(t) &= [\sin(t) \cos(t) 0 0 0 0]^T \text{ if } t \leq 10 \\ r(t) &= [0 1.5 0 0 0 0]^T \text{ if } 10 < t \leq 20 \\ r(t) &= \{\sin(t) \cos(t) + 6.5 0 0 0 0\} \text{ if } 20 < t. \end{aligned}$$

The results of these three simulations are shown in Fig. 3, Fig. 4 and Fig. 5, respectively. Additionally, we see that in Fig. 6, Fig. 7, and Fig. 8 that the gains reach a steady state value.

These figures demonstrate that system stability is achieved in addition to tracking. The variety of signals simulated demonstrate the robustness of our controller design.

IV. NONLINEAR SYSTEM WITH LINEAR CONTROL

In this section, we describe the behavior of the full system (i.e. including nonlinearities), when we attempt to stabilize the system with **linear** feedback (LQR) controller and a **linear** adaptive controller. As expected, the full system dynamic's response is unstable. This is due to the fact

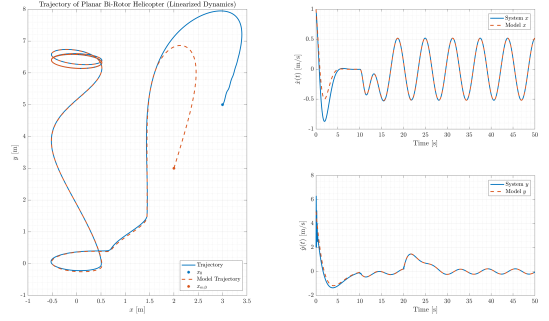


Fig. 5. Bi-Rotor Helicopter Response using a linear adaptive controller and sequential $r(t)$. The system has been stabilized and tracking is achieved.

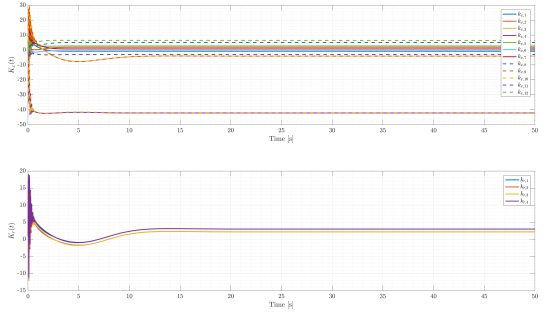


Fig. 6. In this project, the gains $k_x(t)$ and $k_r(t)$ are matrices whose individual values over time are shown. Here, we see that each element of the matrix reaches a steady state value. These are the gain values for the linearized system when tracking a constant reference.

our controllers cannot adequately overcome the system's nonlinearities, causing an inability to achieve tracking, and increasing error over time (i.e., $|e(t)| \rightarrow \infty$). Fig. 9 and Fig. 10 illustrate the divergent behavior of these two cases. We omit the presentation of the gains which were presented in the first submission via canvas (i.e., Phase 1 report) due to space constraints. However, it is worth noting that the gain matrix elements $k_{x,ij} \in K_x(t)$ and $k_{r,ij} \in K_r(t)$ exhibit $|k_{x,ij}| \rightarrow \infty$ and $|k_{r,ij}| \rightarrow \infty$ as $t \rightarrow \infty$.

V. FULL DYNAMICS WITH ADAPTIVE CONTROL UNDER A COORDINATE TRANSFORMATION

In this section we address Phase 2 of the bi-rotor helicopter project which seeks to control the bi-rotor helicopter via a coordinate transformation akin to controlling a point above the helicopter. New equations of motion can be derived by applying the transformation of coordinates to the system shown in (3), where $q = \begin{bmatrix} x \\ y \end{bmatrix}$ and $q' = \begin{bmatrix} x' \\ y' \end{bmatrix}$.

$$q = q + \lambda e_2(\theta) \implies q = q' - \lambda e_2(\theta) \quad (3)$$

Here, we can first define a relationship between $e_1(\theta) = \begin{bmatrix} \cos(\theta) \\ \sin(\theta) \end{bmatrix}$ and $e_2(\theta) = \begin{bmatrix} -\sin(\theta) \\ \cos(\theta) \end{bmatrix}$. With these definitions we can establish useful relationships outlined in (4) and (5).

$$\dot{e}_1(\theta) = \begin{bmatrix} -\sin(\theta)\dot{\theta} \\ \cos(\theta)\dot{\theta} \end{bmatrix} = \begin{bmatrix} -\sin(\theta) \\ \cos(\theta) \end{bmatrix} \dot{\theta} = e_2(\theta)\dot{\theta} \quad (4)$$

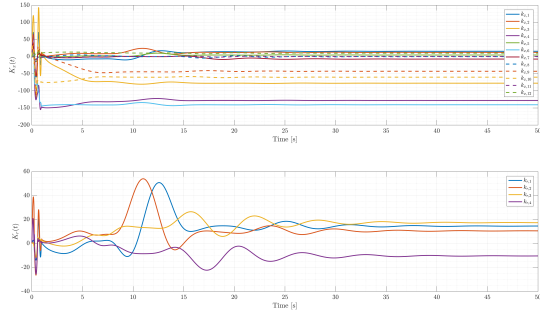


Fig. 7. In this project, the gains $k_x(t)$ and $k_r(t)$ are matrices whose individual values over time are shown. Here, we see that each element of the matrix reaches a steady state value. These are the gain values for the linearized system when tracking a sinusoidal reference.

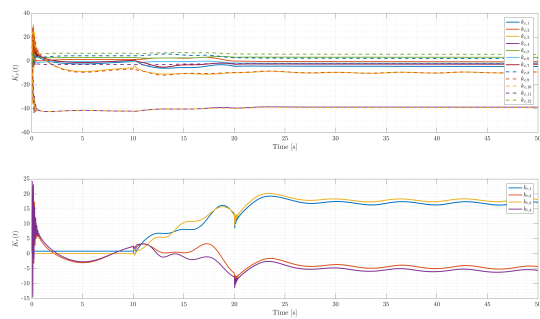


Fig. 8. Adaptation gains for the linearized system, when using sequential signal. The gains $k_x(t)$ and $k_r(t)$ are matrices whose individual values over time are shown. Here, we see that each element of the matrix reaches a steady state value. These are the gain values for the linearized system when tracking a sequential reference.

$$\dot{e}_2(\theta) = \begin{bmatrix} -\cos(\theta)\dot{\theta} \\ -\sin(\theta)\dot{\theta} \end{bmatrix} = \begin{bmatrix} -\cos(\theta) \\ -\sin(\theta) \end{bmatrix} \dot{\theta} = -e_1(\theta)\dot{\theta} \quad (5)$$

Taking the second time derivative yields the definitions in (6) and (7).

$$\ddot{e}_1(\theta) = \begin{bmatrix} -\cos(\theta)\dot{\theta}^2 - \sin(\theta)\ddot{\theta} \\ -\sin(\theta)\dot{\theta}^2 + \cos(\theta)\ddot{\theta} \end{bmatrix} = -e_1(\theta)\dot{\theta}^2 + e_2(\theta)\ddot{\theta} \quad (6)$$

$$\ddot{e}_2(\theta) = \begin{bmatrix} \sin(\theta)\dot{\theta}^2 - \cos(\theta)\ddot{\theta} \\ -\cos(\theta)\dot{\theta}^2 - \sin(\theta)\ddot{\theta} \end{bmatrix} = -e_2(\theta)\dot{\theta}^2 - e_1(\theta)\ddot{\theta} \quad (7)$$

Next, we can define the time derivatives of the system transformation outlined in (8) and (9).

$$\dot{q} = \dot{q}' - \lambda \dot{e}_2(\theta) \quad (8)$$

$$\ddot{q} = \ddot{q}' - \lambda \ddot{e}_2(\theta) \quad (9)$$

Substituting these definitions into our bi-rotor equations of motion yields the following algebraic manipulations.

$$m\ddot{q} = -d\dot{q} + e_2(\theta)[1 \ 1]\vec{f} - mg \quad (10)$$

$$\dot{q}' = -\frac{d}{m}\left(\dot{q}' + \lambda e_1(\theta)\dot{\theta}\right) + \frac{e_2(\theta)}{m}[1 \ 1]\vec{f} - g - \lambda e_2(\theta)\dot{\theta}^2 - \lambda e_1(\theta)\ddot{\theta}$$

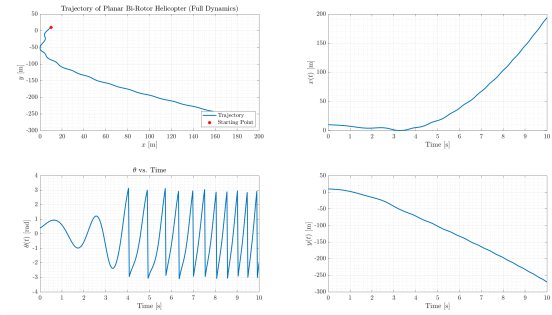


Fig. 9. Closed-Loop Bi-Rotor Helicopter Response, when testing LQR controller on the full nonlinear system. This shows that the nonlinear system has not been stabilized.

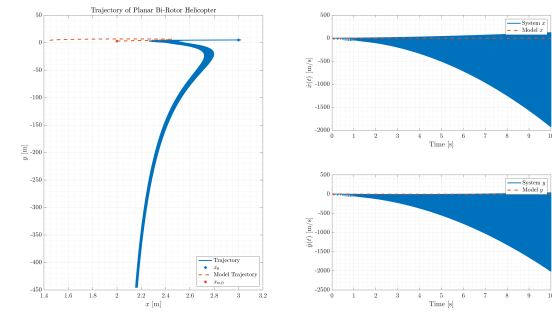


Fig. 10. Closed-Loop Bi-Rotor Helicopter Response, when testing linear adaptive controller on the full nonlinear system. This shows that tracking is not achieved.

Next, we can substitute the definition of $\ddot{\theta}$ from the write-up and consolidate $e_1(\theta)$ and $e_2(\theta)$ into a matrix.

$$\begin{aligned} \ddot{q}' &= -\frac{d}{m}\dot{q}' - \lambda e_2(\theta)\dot{\theta}^2 - \frac{d\lambda}{m}e_1(\theta)\dot{\theta} - \frac{\lambda r}{J}e_1(\theta)[1 \ -1]\vec{f} + \frac{e_2(\theta)}{m}[1 \ 1]\vec{f} - \vec{g} \\ &= -\frac{d}{m}\dot{q}' - \begin{bmatrix} \cos(\theta) & -\sin(\theta) \\ \sin(\theta) & \cos(\theta) \end{bmatrix} \begin{bmatrix} \frac{d\lambda}{m}\dot{\theta} \\ \lambda\dot{\theta}^2 \end{bmatrix} - \begin{bmatrix} \cos(\theta) & -\sin(\theta) \\ \sin(\theta) & \cos(\theta) \end{bmatrix} \begin{bmatrix} \frac{\lambda r}{J} \\ -\frac{1}{m} \end{bmatrix} \vec{f} - \vec{g} \end{aligned}$$

Finally, using the definition of $R(\theta)$ yields the final compact form shown in (10).

$$\ddot{q}' = -\frac{d}{m}\dot{q}' - \lambda R(\theta) \begin{bmatrix} \frac{d}{m}\dot{\theta} \\ \dot{\theta}^2 \end{bmatrix} - R(\theta) \begin{bmatrix} \frac{\lambda r}{J} & -\frac{\lambda r}{m} \\ -\frac{1}{m} & -\frac{1}{m} \end{bmatrix} \vec{f} - \vec{g} \quad (10)$$

Here, we can convert the full system into standard state space form with the following substitutions:

$$\begin{array}{ll} \tilde{x}_1 = x' & \tilde{x}_4 = \dot{y}' \\ \tilde{x}_2 = \dot{x}' & \tilde{x}_5 = \theta \\ \tilde{x}_3 = y' & \tilde{x}_6 = \dot{\theta} \end{array}$$

Additionally, we have the fact that $q' = \begin{bmatrix} x' \\ y' \end{bmatrix}$. Furthermore, we separate the linear and non-linear terms which leads to

$$\begin{aligned} \begin{bmatrix} \dot{\tilde{x}}_1 \\ \dot{\tilde{x}}_2 \\ \dot{\tilde{x}}_3 \\ \dot{\tilde{x}}_4 \\ \dot{\tilde{x}}_5 \\ \dot{\tilde{x}}_6 \end{bmatrix} &= \begin{bmatrix} 0 & 1 & 0 & 0 & 0 & 0 \\ 0 & -\frac{d}{m} & 0 & 0 & 0 & 0 \\ 0 & 0 & 0 & 1 & 0 & 0 \\ 0 & 0 & 0 & -\frac{d}{m} & 0 & 0 \\ 0 & 0 & 0 & 0 & 0 & 1 \\ 0 & 0 & 0 & 0 & 0 & 0 \end{bmatrix} \begin{bmatrix} \tilde{x}_1 \\ \tilde{x}_2 \\ \tilde{x}_3 \\ \tilde{x}_4 \\ \tilde{x}_5 \\ \tilde{x}_6 \end{bmatrix} \\ &+ \begin{bmatrix} 0 \\ -\frac{d\lambda}{m} \cos(\tilde{x}_5) \tilde{x}_6 + \lambda \sin(\tilde{x}_5) \tilde{x}_6^2 - \frac{\lambda r}{m} \cos(\tilde{x}_5)(f_1 - f_2) - \frac{1}{m} \sin(\tilde{x}_5)(f_1 + f_2) \\ 0 \\ -\frac{d\lambda}{m} \sin(\tilde{x}_5) \tilde{x}_6 - \lambda \cos(\tilde{x}_5) \tilde{x}_6^2 - \frac{\lambda r}{m} \sin(\tilde{x}_5)(f_1 - f_2) + \frac{1}{m} \cos(\tilde{x}_5)(f_1 + f_2) \\ 0 \\ \frac{r}{J}(f_1 - f_2) \end{bmatrix} \\ &- \begin{bmatrix} 0 \\ 0 \\ 0 \\ g \\ 0 \\ 0 \end{bmatrix} \end{aligned}$$

It follows:

$$\begin{aligned} \begin{bmatrix} \dot{\tilde{x}}_1 \\ \dot{\tilde{x}}_2 \\ \dot{\tilde{x}}_3 \\ \dot{\tilde{x}}_4 \\ \dot{\tilde{x}}_5 \\ \dot{\tilde{x}}_6 \end{bmatrix} &= \underbrace{\begin{bmatrix} 0 & 1 & 0 & 0 & 0 & 0 \\ 0 & -\frac{d}{m} & 0 & 0 & 0 & 0 \\ 0 & 0 & 0 & 1 & 0 & 0 \\ 0 & 0 & 0 & -\frac{d}{m} & 0 & 0 \\ 0 & 0 & 0 & 0 & 0 & 1 \\ 0 & 0 & 0 & 0 & 0 & 0 \end{bmatrix}}_A \begin{bmatrix} \tilde{x}_1 \\ \tilde{x}_2 \\ \tilde{x}_3 \\ \tilde{x}_4 \\ \tilde{x}_5 \\ \tilde{x}_6 \end{bmatrix} \\ &+ \underbrace{\begin{bmatrix} 0 & 0 & 0 & 0 & 0 & 0 \\ 0 & \cos(\tilde{x}_5) & 0 & -\sin(\tilde{x}_5) & 0 & 0 \\ 0 & 0 & 0 & 0 & 0 & 0 \\ 1 & \sin(\tilde{x}_5) & 0 & \cos(\tilde{x}_5) & 0 & 0 \\ 0 & 0 & 0 & 0 & 0 & 0 \\ 0 & 0 & 0 & 0 & 0 & 1 \end{bmatrix}}_B \times \\ &\quad \underbrace{\begin{bmatrix} -\frac{d\lambda}{m} \tilde{x}_6 - \frac{-\lambda r}{J} [1 & -1] \vec{f} \\ -\lambda \tilde{x}_6^2 + \frac{1}{m} [1 & 1] \vec{f} \\ \frac{r}{J} [1 & -1] \vec{f} \end{bmatrix}}_{\Phi(x(t))} \end{aligned}$$

Further expanding the matrix leads to

$$\begin{aligned} \begin{bmatrix} \dot{\tilde{x}}_1 \\ \dot{\tilde{x}}_2 \\ \dot{\tilde{x}}_3 \\ \dot{\tilde{x}}_4 \\ \dot{\tilde{x}}_5 \\ \dot{\tilde{x}}_6 \end{bmatrix} &= \underbrace{\begin{bmatrix} 0 & 1 & 0 & 0 & 0 & 0 \\ 0 & -\frac{d}{m} & 0 & 0 & 0 & 0 \\ 0 & 0 & 0 & 1 & 0 & 0 \\ 0 & 0 & 0 & -\frac{d}{m} & 0 & 0 \\ 0 & 0 & 0 & 0 & 0 & 1 \\ 0 & 0 & 0 & 0 & 0 & 0 \end{bmatrix}}_A \begin{bmatrix} \tilde{x}_1 \\ \tilde{x}_2 \\ \tilde{x}_3 \\ \tilde{x}_4 \\ \tilde{x}_5 \\ \tilde{x}_6 \end{bmatrix} \\ &+ \underbrace{\begin{bmatrix} 0 & 0 & 0 & 0 & 0 & 0 \\ 0 & \cos(\tilde{x}_5) & 0 & -\sin(\tilde{x}_5) & 0 & 0 \\ 0 & 0 & 0 & 0 & 0 & 0 \\ 1 & \sin(\tilde{x}_5) & 0 & \cos(\tilde{x}_5) & 0 & 0 \\ 0 & 0 & 0 & 0 & 0 & 0 \\ 0 & 0 & 0 & 0 & 0 & 1 \end{bmatrix}}_B \times \\ &\quad \underbrace{\begin{bmatrix} 0 & 0 & 0 & 0 & 0 & 0 \\ -\frac{\lambda r}{J} & \frac{\lambda r}{J} & 0 & 0 & 0 & 0 \\ 0 & 0 & 0 & 0 & 0 & 0 \\ \frac{1}{m} & \frac{1}{m} & 0 & 0 & 0 & 0 \\ 0 & 0 & 0 & 0 & 0 & 0 \\ -\frac{r}{J} & \frac{r}{J} & 0 & 0 & 0 & 0 \end{bmatrix}}_{u(t)=C\vec{f}} \underbrace{\begin{bmatrix} -g & 0 & 0 & 0 & 0 & 0 \\ 0 & -\frac{d\lambda}{m} & 0 & 0 & 0 & 0 \\ 0 & 0 & 0 & 0 & 0 & 0 \\ 0 & 0 & 0 & -\lambda & 0 & 0 \\ 0 & 0 & 0 & 0 & 0 & 0 \\ 0 & 0 & 0 & 0 & 0 & 0 \end{bmatrix}}_{\vec{f}^T} \underbrace{\begin{bmatrix} 1 \\ \tilde{x}_6 \\ \tilde{x}_6^2 \\ \tilde{x}_6 \\ 0 \\ 0 \end{bmatrix}}_{\Phi(x(t))} \end{aligned}$$

We conclude that the dynamics of the transformed system above can be converted to the general form covered in class

$$\dot{\tilde{x}} = A\tilde{x} + B(u(t) + \alpha^T \Phi(x(t)))$$

It should be noted that the controller of our original system is \vec{f} . Here, we instead perform a transformation and take the new controller to be $u(t) = C\vec{f}$, so we are not directly designing the forces that will be applied on the helicopter. Since we multiply the real controller (\vec{f}) by the C matrix, obtaining $u(t)$, the dimension of the controller we design in this step is different from the dimension of the controller we define for the linearized system. This implies that, based on how the controller is defined, the reference signals have a different dimension as well. Lastly, we look for $u(t)$ using

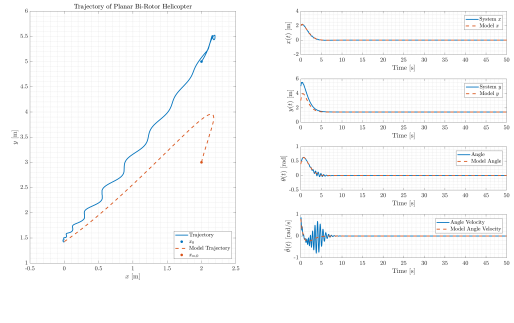


Fig. 11. Trajectory of the system for $r(t) = [2 \ 0 \ 2 \ 0 \ 0 \ 0]^T$. Tracking is achieved and the system is stable. $\theta \rightarrow 0$ as we wanted.

our adaptive techniques but find the \vec{f} using the pseudo-inverse of C . The matrix C is found two equations before this paragraph.

After we stabilize the system with the transformed controller, we then apply the inverse transformation to ensure that our original controller \vec{f} satisfies the specifics of this project. To do so, we design an adaptive controller with input constraints. The equations for our system are the following

$$\text{Plant: } \dot{\tilde{x}} = A\tilde{x} + B(u_c(t) + \Delta u + \alpha^T \Phi(x(t)))$$

$$\text{Controller: } u_c(t) = k_x^T(t)\tilde{x}(t) + k_r^T(t)r(t) - \hat{\alpha}^T \Phi(x(t))$$

$$\text{Reference: } \dot{x}_m = A_m x_m(t) + B_m r(t) + B_m k_u(t) \Delta u$$

where $\Delta u = u - u_c$ and

$$u(t) = u_{max} \text{sat} \left(\frac{u_c(t)}{u_{max}} \right)$$

The adaptive laws are:

$$\dot{k}_x = -\Gamma_x \tilde{x}(t) e^T P B \text{sign}(\lambda)$$

$$\dot{k}_r = -\Gamma_r r(t) e^T P B \text{sign}(\lambda)$$

$$\dot{k}_u = \Gamma_u \Delta u e^T P B_m$$

$$\dot{\hat{\alpha}} = \Gamma_\alpha \Phi(x(t)) e^T P B \text{sign}(\lambda)$$

Lastly, the model A_m is found by using pole placement with the care() MATLAB function. We take $B_m = B$ for these cases as well.

Three main cases of interest are described.

- Tracking of a linear trajectory, $r(t)$ is a constant
- Tracking of a circular trajectory, $r(t)$ is a sinusoid
- Tracking of a signal changing over time trajectory (Sequential Reference)

A. Constant Reference

For this test we utilized the following reference signal

$$r(t) = [2 \ 0 \ 2 \ 0 \ 0 \ 0]^T$$

Results of the simulation for this case of interest are shown in Fig. 11, Fig. 12, Fig. 13 and Fig. 14.

B. Sinusoidal Reference

For this test we utilized the following reference signal

$$r(t) = [\sin(t) \ \cos(t) \ 2 \ 0 \ 0 \ 0]^T$$

Results of the simulation for this case of interest are shown in Fig. 15, Fig. 16, Fig. 17 and Fig. 18.

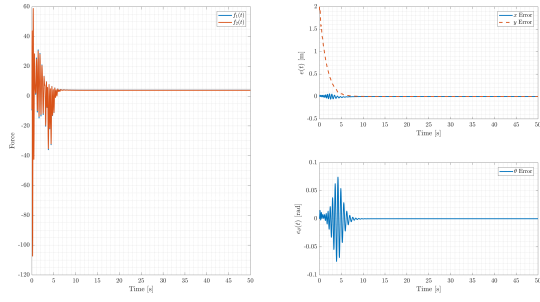


Fig. 12. Left: Force applied on the system. As we notice the constraint imposed on the force is satisfied. Right: error is going to zero, so tracking is achieved

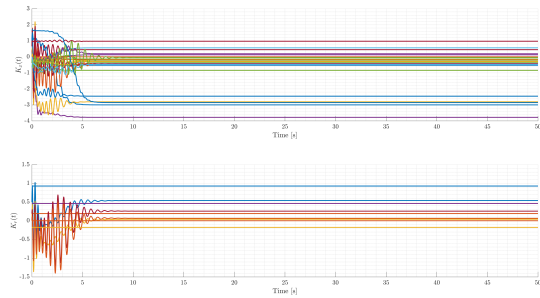


Fig. 13. $k_x(t)$ and $k_r(t)$ to show that we have bounded gains and the system is not blowing up.

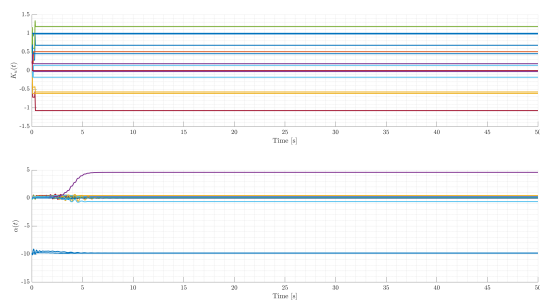


Fig. 14. $k_u(t)$ and $\hat{\alpha}(t)$ to show that we have bounded gains and the system is not blowing up.

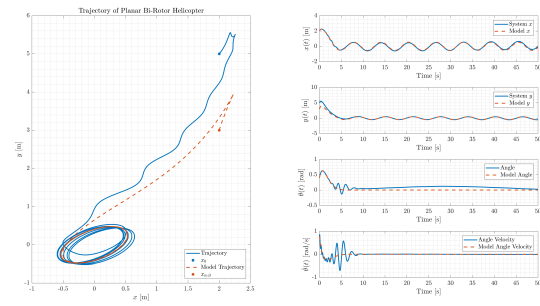


Fig. 15. Trajectory of the system for $r(t) = [\sin(t) \cos(t) 0 0 0 0]^T$. Tracking is achieved and the system is stable. $\theta \rightarrow 0$ as we wanted.

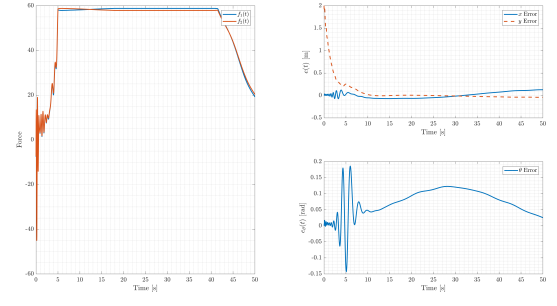


Fig. 16. Left: Force applied on the system. As we notice the constraint imposed on the force is satisfied. Right: error is going to zero, so tracking is achieved

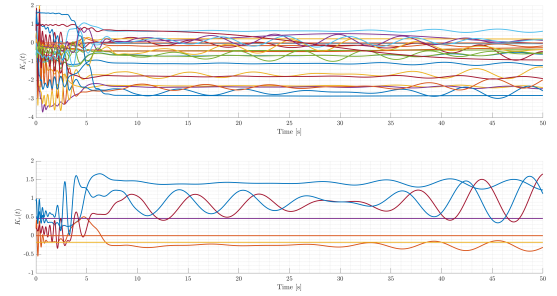


Fig. 17. $k_x(t)$ and $k_r(t)$ to show that we have bounded gains and the system is not blowing up.

C. Sequential Reference

Like for the linearized system, we chose to do an additional test of our adaptive control method which switches references signals at specific points in time, to fully illustrate the capabilities on the adaptive system. The sequence of signals are as follows

$$\begin{aligned} r(t) &= [2 \ 0 \ 0 \ 0 \ 0 \ 0]^T \quad \text{if } t \leq 3 \\ r(t) &= [\sin(t) \ \cos(t) \ 0 \ 0 \ 0 \ 0]^T \quad \text{if } 3 < t \leq 30 \\ r(t) &= [\sin(t) + 5 \ \cos(t) + 5 \ 0 \ 0 \ 0 \ 0]^T \quad \text{if } t > 30 \end{aligned}$$

Results of the simulation for this case of interest are shown in Fig. 19, Fig. 20, Fig. 21 and Fig. 22.

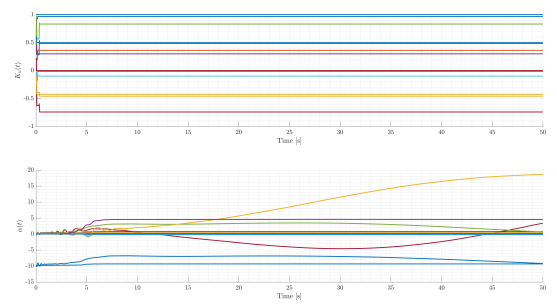


Fig. 18. $k_u(t)$ and $\hat{\alpha}(t)$ to show that we have bounded gains and the system is not blowing up.

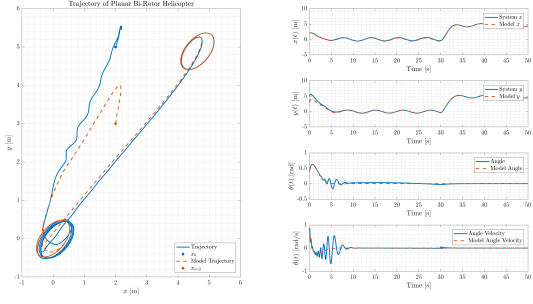


Fig. 19. Trajectory of the system for sequential reference. Tracking is achieved and the system is stable. $\theta \rightarrow 0$ as we wanted.

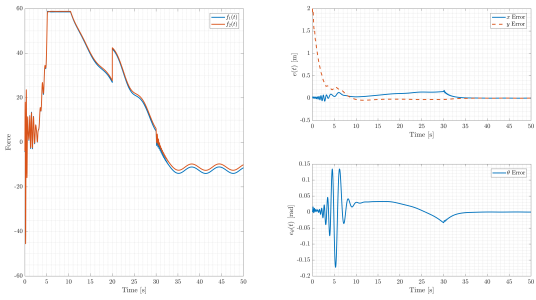


Fig. 20. Left: Force applied on the system. As we notice the constraint imposed on the force is satisfied. Right: error is going to zero, so tracking is achieved

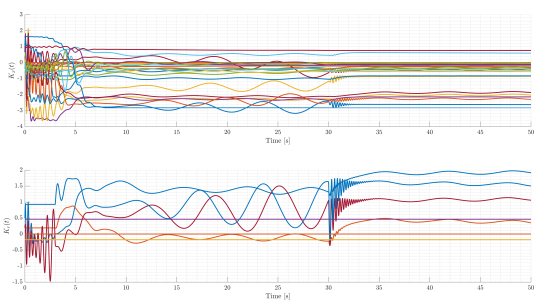


Fig. 21. $k_x(t)$ and $k_r(t)$ to show that we have bounded gains and the system is not blowing up.

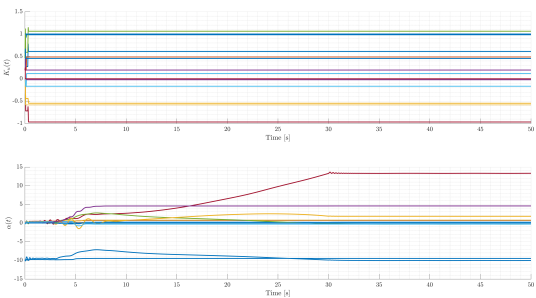


Fig. 22. $k_u(t)$ and $\alpha(t)$ to show that we have bounded gains and the system is not blowing up.

VI. CONCLUSIONS

This project is comprised of two phases where we address the problems of stability and tracking of reference signals. Additionally, we demonstrate the limitations of the linear controllers.

In Phase 1, we linearize the dynamics about the $x_5 = 0$ point. From this linearization we are able to design an LQR controller and a linear adaptive controller. With our adaptive controller, we are able to achieve tracking of a variety of signals (i.e., constant, sinusoidal, and signal switching sequence). Further investigation of our controller led us to apply these techniques to the full dynamics including the nonlinearities. The system behaves as expected. In other words, we see that the linear controllers are insufficient for stabilizing the full system dynamics or to achieve tracking.

In Phase 2, we tackle the problem of adaptive control with full system dynamics (i.e., including nonlinearities) via a coordinate transformation. The coordinate transformation leads to a concise manner of representing the full system dynamics leading to a form we are familiar with from class (i.e., nonlinearities in the span of the input space). Our approaches to stabilization and tracking of various signals (i.e., constant, sinusoidal, and signal switching sequence) for a bi-rotor helicopter are shown to be successful. We also note that the adaptive controller which has non-linearities performs much better at stabilizing and achieving tracking in our system than the linear controller from Phase 1. This behavior makes sense since we are now able to better mitigate for the growth of nonlinearities in the system.

Overall, we present successful tracking in both Phase 1 & 2 of this project while also highlight the limitations of the linear controllers in Phase 1 and improved ways of performing tracking in Phase 2.